

# **Sigma-omega meson coupling and properties of nuclei and nuclear matter**

Maryam M. Haidari and Madan M. Sharma

*Physics Department, Kuwait University, Kuwait 13060*

(Dated: February 9, 2020)

## **Abstract**

We have constructed a Lagrangian model (SIG-OM) with coupling of  $\sigma$  and  $\omega$  mesons in the relativistic mean-field theory. Properties of finite nuclei and nuclear matter have been explored with the new Lagrangian. The study shows that with SIG-OM an excellent description of binding energies and charge radii of nuclei over a large range of isospin is achieved. With an incompressibility of nuclear matter  $K = 265$  MeV, it is also able to describe the breathing-mode isoscalar giant monopole resonance energies successfully. It is shown that the high-density behaviour of the equation of state of nuclear and neutron matter with the  $\sigma$ - $\omega$  coupling is significantly softer than that of the non-linear scalar coupling model.

PACS numbers: 21.30.Fe, 21.10.Dr, 21.60.-n, 24.10.Cn, 24.10.Jv, 21.65.+f

arXiv:nucl-th/0702001v2 22 May 2007

## I. INTRODUCTION

The relativistic mean-field (RMF) theory [1, 2, 3] has been a successful approach to describing properties of nuclei along the stability line as well as far away from it [4, 5, 6]. Due to the Dirac-Lorentz structure of spin-orbit interaction, it has been advantageous over the conventional non-relativistic Skyrme theory in describing properties such as anomalous isotope shifts in Pb nuclei [7]. It was shown [8] that an isospin dependence of the spin-orbit interaction is responsible for the anomalous behaviour of the isotope shifts. On the other hand, by significant alterations in the isospin dependence of the spin-orbit potential in the Skyrme theory [8, 9], it has become possible to describe the above anomaly in isotope shifts.

The prevalent model within the RMF theory is that of non-linear couplings of  $\sigma$  meson [10]. One of the first successful nuclear forces within this model has been NL-SH [5]. An improved version of this model has brought out the set NL3 [6]. The model with  $\sigma^3 + \sigma^4$  is, however, beset with the disadvantage that it gives an equation of state (EOS) of nuclear and neutron matter that is very stiff and is consequently not commensurate with the observed neutron star masses. Recently, a quartic term  $\omega^4$  was added to the above model that was intended to improve the shell effects in nuclei [11]. The addition of vector self-coupling of  $\omega$  meson has the advantage of softening the EOS of nuclear matter.

With the success of the RMF theory in nuclear structure, there has been a desire to construct a theory that is appropriate for broader aspects of finite nuclei as well as for nuclear matter. Variations in the relativistic approach based upon point-coupling model [12, 13] or of density-dependent meson couplings [14, 15, 16, 17] have been made. With the inclusion of a large number of parameters (13 in this case), a moderate success has been achieved [16]. With the inclusion of quartic coupling of  $\omega$  meson, a softer EOS of the nuclear matter has been obtained [18]. There has been significant discussion on the use of the effective field theoretical approach based upon expansion of the interaction Lagrangian in higher order terms in fields [19, 20, 21]. Addition of higher order terms and cross terms between the fields are shown to improve description of properties of finite nuclei [20, 22]. Recently, a coupling between  $\sigma$  and  $\rho$  meson has shown to be promising in reduction of neutron skin to reasonably accepted values as well as for obtaining a softer EOS of nuclear matter [22].

As improved and refined predictions of nuclear properties especially the masses (binding

energies) of nuclei are required in regions often very far away from the stability line, it has become pertinent to devise new and improved methods and approaches to deliver the same. In this work, we have explored the RMF Lagrangian in the effective field theoretical approach with a limited number of terms in the expansion. We have restricted ourselves to a cross term between  $\sigma$  and  $\omega$  mesons. Specifically, we have added a coupling of the form  $\sigma^2\omega^2$ , in addition to the  $\sigma^3 + \sigma^4$  couplings.

## II. FORMALISM

The RMF Lagrangian that describes nucleons as Dirac spinors moving in the meson fields is given by [1]

$$\begin{aligned} \mathcal{L} = & \bar{\psi} \left( \not{p} - g_\omega \not{\psi} - g_\rho \not{\vec{\rho}} - \frac{1}{2}e(1 - \tau_3)A - g_\sigma \sigma - M_N \right) \psi \\ & + \frac{1}{2} \partial_\mu \sigma \partial^\mu \sigma - U(\sigma) - \frac{1}{4} \Omega_{\mu\nu} \Omega^{\mu\nu} + \frac{1}{2} m_\omega^2 \omega_\mu \omega^\mu \\ & - \frac{1}{4} \vec{R}_{\mu\nu} \vec{R}^{\mu\nu} + \frac{1}{2} m_\rho^2 \vec{\rho}_\mu \vec{\rho}^\mu - \frac{1}{4} F_{\mu\nu} F^{\mu\nu} \end{aligned} \quad (1)$$

where  $M_N$  is the bare nucleon mass and  $\psi$  is its Dirac spinor. Nucleons interact with  $\sigma$ ,  $\omega$ , and  $\rho$  mesons, with coupling constants being  $g_\sigma$ ,  $g_\omega$ , and  $g_\rho$ , respectively. The photonic field is represented by the electromagnetic vector  $A^\mu$ . The nonlinear  $\sigma$ -meson-couplings and the  $\sigma$ - $\omega$  coupling are given by

$$U_{NL} = \frac{1}{2} m_\sigma^2 \sigma^2 + \frac{1}{3} g_2 \sigma^3 + \frac{1}{4} g_3 \sigma^4 - \frac{1}{2} g_{\sigma\omega} \sigma^2 \omega_\mu \omega^\mu. \quad (2)$$

The parameters  $g_2$  and  $g_3$  are the nonlinear couplings of  $\sigma$ -meson in the conventional  $\sigma^3 + \sigma^4$  model. The constant  $g_{\sigma\omega}$  represents the coupling between  $\sigma$  and  $\omega$  meson introduced herein. The corresponding Klein-Gordan equations are written as

$$(-\Delta + m_\sigma^{*2})\sigma = -g_\sigma \bar{\psi} \psi \quad (3)$$

$$(-\Delta + m_\omega^{*2})\omega_\nu = g_\omega \bar{\psi} \gamma_\nu \psi \quad (4)$$

$$(-\Delta + m_\rho^2)\vec{\rho}_\nu = g_\rho \bar{\psi} \gamma_\nu \vec{\tau} \psi \quad (5)$$

$$-\Delta A_\nu = \frac{1}{2} e \bar{\psi} (1 + \tau_3) \gamma_\nu \psi, \quad (6)$$

where,

$$m_{\sigma}^{*2} = m_{\sigma}^2 + g_2\sigma + g_3\sigma^2 - g_{\sigma\omega}\omega_0^2 \quad (7)$$

$$m_{\omega}^{*2} = m_{\omega}^2 + g_{\sigma\omega}\sigma^2 \quad (8)$$

These equations imply an implicit density dependence of  $\sigma$  and  $\omega$  meson masses.

### III. THE LAGRANGIAN SET

The parameters of the new Lagrangian model are obtained by fitting binding energies and charge radii of a set of nuclei as described in ref. [5]. The nuclei included are  $^{16}\text{O}$ ,  $^{40}\text{Ca}$ ,  $^{90}\text{Zr}$ ,  $^{116}\text{Sn}$ ,  $^{124}\text{Sn}$  and  $^{208}\text{Pb}$ . The Sn isotopes of  $^{116}\text{Sn}$  and  $^{124}\text{Sn}$  are included with a view to take into account the required isospin dependence. In addition, we have tagged the spin-orbit splitting of  $p_{3/2} - p_{1/2}$  in  $^{16}\text{O}$ . No explicit conditions have been put on the nuclear matter properties. The  $\omega$  and  $\rho$  meson masses have been fixed at the empirical values.

The parameters of the Lagrangian thus obtained (named as SIG-OM) are listed in Table 1. These are compared with those of the forces NL-SH and NL3. The coupling constant  $g_3$  is positive in contrast with that of NL-SH and NL3, where it is predominantly negative. It has been noted [2] that the negative  $g_3$  has a consequence in that the spectrum of the full theory is not bound from below and that renormalization of the scalar field is not possible.

Solving the equations for nuclear matter at the saturation point, equilibrium properties of the nuclear matter are calculated. Nuclear properties arising from the parameters of SIG-OM are shown at the bottom of Table 1 and are compared with those of NL-SH and NL3. The saturation density and binding energy per nucleon for SIG-OM are very close to those of NL-SH and NL3 and are in physically acceptable region. The incompressibility of nuclear matter  $K$  that arises from SIG-OM is 265.2 MeV. It is slightly smaller than that of NL3 ( $K = 271.6$  MeV). The effective mass at the saturation point is  $m^* = 0.62$  with SIG-OM. It is slightly bigger than a value of  $\sim 0.60$  for NL-SH and NL3. The asymmetry energy  $a_4$  of SIG-OM is 37.0 MeV. It is comparable to that of NL-SH and NL3 and is, however, still bigger than the received empirical value of  $\sim 33$  MeV.

TABLE I: The parameters and nuclear matter properties of the force SIG-OM with the coupling between  $\sigma$  and  $\omega$  meson. The Lagrangian sets with the non-linear scalar self-coupling NL-SH, NL3 are also shown for comparison

Parameters	SIG-OM	NL-SH	NL3
$M$ (MeV)	939.0	939.0	939.0
$m_\sigma$ (MeV)	505.9263	526.0592	508.1941
$m_\omega$ (MeV)	783.0	783.0	782.501
$m_\rho$ (MeV)	763.0	763.0	763.0
$g_\sigma$	10.0430	10.4436	10.2169
$g_\omega$	12.7669	12.9451	12.8675
$g_\rho$	4.4751	4.3828	4.4744
$g_2$ (fm $^{-1}$ )	-7.9233	-6.9099	-10.4307
$g_3$	12.4600	-15.8337	-28.8851
$g_{\sigma\omega}$	35.6924	0.0	0.0
Nuclear matter properties			
$\rho_0$ (fm $^{-3}$ )	0.149	0.146	0.148
$a_v$ (MeV)	-16.30	-16.33	-16.24
$K$ (MeV)	265.2	354.9	271.6
$m^*$	0.622	0.597	0.595
$a_4$ (MeV)	37.0	36.1	37.4

#### IV. RESULTS AND DISCUSSION

The binding energies and charge radii of nuclei calculated with SIG-OM are presented in Tables 2 and 3, respectively. Results with NL-SH and NL3 are also given for comparison. Table 2 shows the binding energies of 6 key nuclei included in the fit along with those of several isotopes of Sn and Pb. The experimental binding energies [23] are shown in the last column. The binding energies of 6 nuclei included in the fit are reproduced well by SIG-OM with a slight overbinding for  $^{16}\text{O}$ . The binding energy of other isotopes of Sn and Pb

TABLE II: The binding energy (in MeV) of nuclei calculated with SIG-OM. The values for NL3 and NL-SH are also shown for comparison. The empirical values (exp.) are shown in the last column. The nuclei included in the fit are indicated by an asterix.

Nucleus	SIG-OM	NL-SH	NL3	exp.
$^{16}\text{O}$ (*)	-129.2	-128.4	-128.8	-127.6
$^{40}\text{Ca}$ (*)	-343.3	-340.1	-342.0	-342.1
$^{90}\text{Zr}$ (*)	-783.2	-782.9	-782.6	-783.9
$^{100}\text{Sn}$	-825.9	-830.6	-829.2	-824.5
$^{116}\text{Sn}$ (*)	-988.6	-987.9	-987.7	-988.7
$^{124}\text{Sn}$ (*)	-1049.9	-1050.1	-1050.2	-1050.0
$^{132}\text{Sn}$	-1102.7	-1105.9	-1105.4	-1102.9
$^{202}\text{Pb}$	-1592.6	-1596.0	-1592.6	-1592.2
$^{208}\text{Pb}$ (*)	-1638.2	-1640.4	-1639.6	-1636.7
$^{214}\text{Pb}$	-1663.7	-1664.3	-1661.6	-1663.3

nuclei obtained with SIG-OM show an excellent agreement with the experimental data as compared to NL-SH and NL3. Especially, the doubly magic nucleus  $^{100}\text{Sn}$  is best described by SIG-OM, whereas nearly all other Lagrangian models overestimate its binding energy by  $\sim 4\text{-}5$  MeV.

The charge radii of nuclei calculated with SIG-OM are given in Table 3 and are compared to values obtained with NL-SH and NL3. SIG-OM describes the experimental charge radii very well. In comparison, NL3 tends to overestimate the experimental values of heavy nuclei, as will be shown below for Pb isotopes.

With the new Lagrangian model SIG-OM, we have performed a case study in order to test its prediction capabilities. The isotopic chain of Sn with its experimental masses available from the proton drip-line doubly magic nucleus  $^{100}\text{Sn}$  to another doubly magic nucleus  $^{132}\text{Sn}$  offers unique data for a complete coverage of the shell from  $N = 50$  to  $N = 82$ . The binding energies of Sn nuclei obtained with SIG-OM are shown in Fig. 1 and are compared with

TABLE III: The rms charge radius (in  $fm$ ) obtained with SIG-OM. The values for NL-SH and NL3 are also shown for comparison. The empirical charge radii (exp.) are shown in the last column.

Nucleus	SIG-OM	NL-SH	NL3	exp.
$^{16}\text{O}$	2.699	2.699	2.728	2.730
$^{40}\text{Ca}$	3.440	3.452	3.470	3.450
$^{90}\text{Zr}$	4.282	4.289	4.287	4.258
$^{116}\text{Sn}$	4.593	4.599	4.599	4.626
$^{124}\text{Sn}$	4.645	4.651	4.661	4.673
$^{208}\text{Pb}$	5.506	5.509	5.523	5.503
$^{214}\text{Pb}$	5.563	5.562	5.581	5.558

those of NL3 and NL-SV1. Here, we have included the results of NL-SV1 [11], which is based upon the quartic coupling of  $\omega$  meson. The results show a significant difference between the predictions of SIG-OM and both the other Lagrangian models in the regions near the closed shells. Both NL3 and NL-SV1 show significant deviations from the experimental values below  $A < 106$ . For the double-magic nucleus  $^{100}\text{Sn}$ , the overbinding amounts to 4-5 MeV. SIG-OM shows an excellent agreement with the experimental data all over the range of the shell. Especially, for nuclei near the closed shell  $N = 50$ , SIG-OM provides the best available description of the binding energies.

The RMF calculations for binding energies of nuclei in the isotopic chain of Pb with SIG-OM also show a good agreement with the experimental values. The results for few a Pb isotopes have been shown in Table 2. The salient feature of the Pb chain is the presence of a characteristic kink in charge radii at the closed shell at  $N = 82$ . This behaviour of charge radii was considered for long to be anomalous.

We show in Fig. 2 the charge radii of Pb isotopes calculated with SIG-OM, NL-SH and NL3. The experimental values [24] are shown for comparison. A kink across  $A = 208$  ( $N = 82$ ) arises in all the curves. The corresponding isotope shifts calculated with the forces considered here produce a kink across the magic number. We note that the RMF theory describes the experimental isotope shifts very well irrespective of the nature of the Lagrangian model employed, with barely perceptible differences amongst various

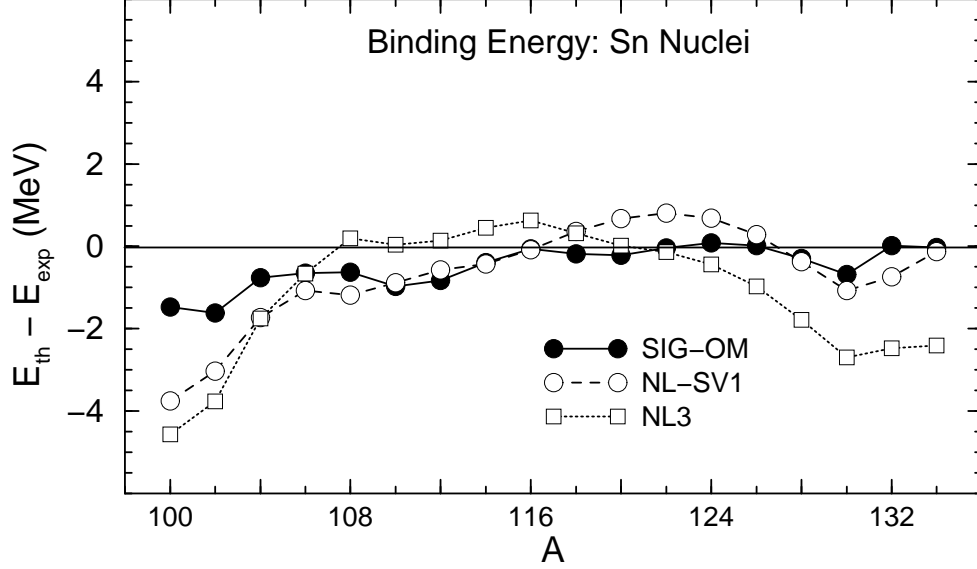


FIG. 1: The binding energies of Sn nuclei obtained with SIG-OM. The results obtained with NL3 and NL-SV1 are also shown for comparison

forces. These are therefore not shown here. In order to view the quality of predictions comparatively, we focus upon the absolute values of charge radii. Here, SIG-OM describes the experimental data as well as NL-SH. For nuclei below  $^{208}\text{Pb}$ , there are minor differences with the experimental data for both SIG-OM and NL-SH. In comparison, NL3 overestimates the charge radii of all the Pb isotopes (see also Table 3).

Mass measurements with high precision on nuclei far away from the stability are being performed at various facilities and new experimental data are emerging currently. Such data provide a crucial test bench for various nuclear models in regions away from the stability line. In order to test the predictive power of the present Lagrangian, we have performed deformed RMF calculations for some nuclei on which experimental data has been obtained recently. The total binding energy of some isotopes of Si, Sr, and Mo and a few others obtained with SIG-OM is shown in Table 4. A comparison is made with NL3. The experimental binding energies obtained from high-precision experimental masses on Si [25], Sr [26]) and Mo [27]) are used for comparison. It is noted that SIG-OM describes the experimental binding energies very well with a few exceptions only. The agreement is especially good for newly measured Si isotopes. The force NL3, on the other hand, shows somewhat larger deviations from the data notably for Si isotopes. Details of a comprehensive study to examine the shell structure of the Lagrangian model SIG-OM encompassing a larger number of recent

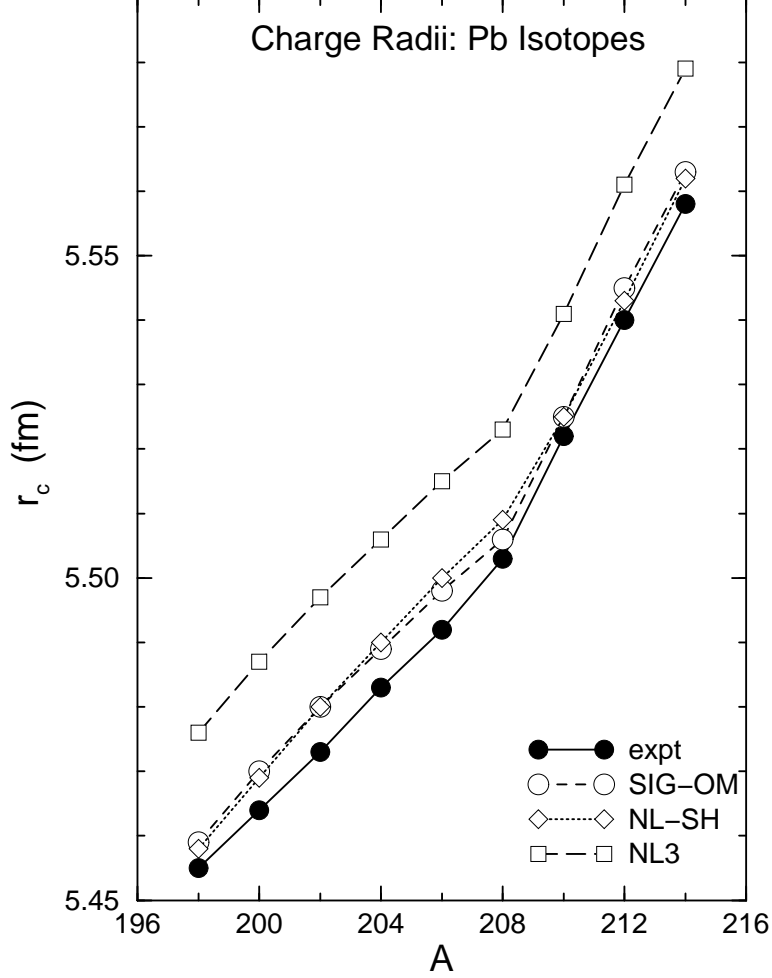


FIG. 2: The charge radii calculated with SIG-OM, NL-SH and NL3. Experimental values are also shown for comparison

data in the regions far away from the stability line will be discussed elsewhere [28].

It may be recalled that within the  $\sigma^3 + \sigma^4$  model, the force NL3 was obtained with a value of incompressibility  $K = 271$  MeV in the range of physically acceptable values. In order to compare the outcome of various Lagrangians on the breathing-mode giant monopole resonance (GMR) energies, we have performed constrained generator coordinate method (GCM) calculations for the GMR mode for a set of nuclei [29]. The nuclei included are  $^{90}\text{Zr}$ ,  $^{120}\text{Sn}$  and  $^{208}\text{Pb}$ . Experimental GMR energies on these nuclei are known with a reasonable precision [30, 31]. The results of our calculations are shown in Table 5 and are compared with the experimental data. Clearly, the force NL-SH ( $K = 355$  MeV) provides larger GMR energies due to its high incompressibility. NL3 ( $K = 271$  MeV), on the other hand,

TABLE IV: The binding energy  $E$  (in MeV) and quadrupole deformation  $\beta_2$  of nuclei away from the stability line calculated with SIG-OM. The deviation of the binding energy from the experimental value,  $\Delta E = E - E_{exp}$ , is also given. The values with NL3 are shown for comparison.

Nucleus	SIG-OM			NL3		
	$E$	$\beta_2$	$\Delta E$	$E$	$\beta_2$	$\Delta E$
$^{36}\text{Si}$	-292.4	0.02	-0.4	-293.5	0.0	-1.5
$^{38}\text{Si}$	-300.0	0.28	-0.2	-301.3	0.27	-1.5
$^{40}\text{Si}$	-306.6	0.36	-0.1	-307.9	0.34	-1.4
$^{42}\text{Si}$	-313.3	-0.35	-0.4	-315.2	-0.33	-2.3
$^{80}\text{Sr}$	-684.8	0.0	+1.5	-682.8	0.0	+3.5
$^{86}\text{Sr}$	-748.9	0.0	0.0	-748.2	0.0	+0.7
$^{88}\text{Sr}$	-768.1	0.0	+0.4	-768.0	0.0	+0.5
$^{108}\text{Mo}$	-909.2	-0.22	+0.4	-908.3	-0.23	+1.3
$^{110}\text{Mo}$	-919.6	-0.23	-0.1	-919.0	-0.23	+0.5
$^{120}\text{Xe}$	-1008.2	0.26	+0.3	-1007.7	0.29	+0.8
$^{174}\text{Yb}$	-1407.2	0.31	-0.6	-1407.2	0.32	-0.6

underestimates the GMR data.

It is interesting to note that SIG-OM with its slightly lower value of  $K = 265$  MeV than that of NL3 provides GMR energies which are in good agreement with the data, especially those of  $^{90}\text{Zr}$  and  $^{208}\text{Pb}$  considered frequently in analyses. On the other hand, NL3 with a higher value  $K = 271$  MeV underestimates the data by  $\sim 1$  MeV. In general, it is known that a force with a lower value of  $K$  would yield smaller values of GMR energies. In view of this, the predictions of SIG-OM and NL3 seem to be rather paradoxical. The apparent paradox can be understood in terms of the surface compressibility. Though NL3 has a value of  $K$  slightly higher than that of SIG-OM, a difference of about 1 MeV in the GMR energies suggests a smaller surface incompressibility coefficient with SIG-OM. Comparatively, a larger negative contribution from the surface term decreases the GMR energies with NL3. A detailed study of this aspect will be presented elsewhere.

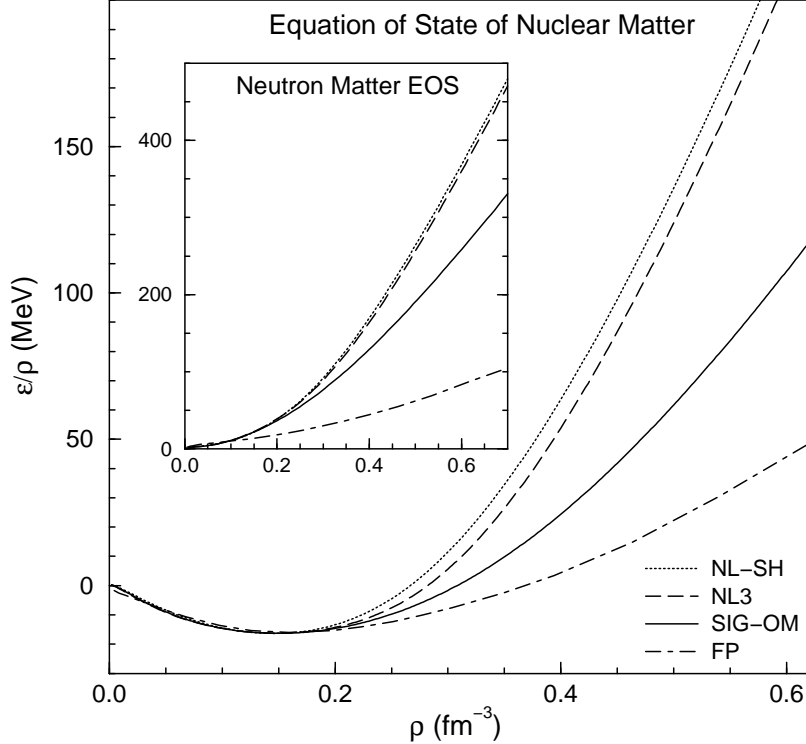


FIG. 3: The equation of state (EOS) of nuclear matter and neutron matter (inset) obtained with SIG-OM, NL-SH and NL3

TABLE V: The breathing mode GMR energies in nuclei obtained with the the constrained generator coordinate method. The experimental data are from refs. [30, 31]

Nucleus	SIG-OM	NL3	NL-SH	exp.
$^{90}\text{Zr}$	18.2	16.9	19.5	$17.81 \pm 0.30$
$^{120}\text{Sn}$	16.2	15.0	16.7	$15.52 \pm 0.15$
$^{208}\text{Pb}$	14.1	13.0	15.0	$13.96 \pm 0.28$

The equation of state (EOS) of nuclear and neutron matter bears significance to structure and properties of neutron stars. Solving the equations for nuclear matter self-consistently, we have calculated the EOS of nuclear and neutron matter. The EOS for SIG-OM shows a significant softening at higher densities, as compared to that of NL-SH and NL3 (see Fig. 3). The coupling of  $\sigma$  and  $\omega$  meson has a softening effect at higher densities. In contrast, EOS with  $\sigma^3 + \sigma^4$  models is notoriously hard due to preponderance of  $\omega$  term at high densities. The corresponding EOS for neutron matter (in inset of Fig. 3) with SIG-OM is also softer

than that for NL-SH and NL3. For comparison, we show the EOS due to Friedman and Padharipande (FP) [32]. The softening achieved by the  $\sigma\omega$  coupling is not strong enough to match that of FP which is a very soft EOS leading to smaller values of maximum mass of neutron stars [32]. Apparently, some other ingredient(s) would be required in order to mock the FP EOS, though our preliminary calculations of neutron-star structure with SIG-OM show that the softening of EOS brings down the maximum neutron-star mass closer to the empirical maximum values.

## V. CONCLUSION

In conclusion, the Lagrangian with the coupling of  $\sigma$  and  $\omega$  mesons that we have developed serves to provide a very good description of the ground-state properties such as binding energies and charge radii of nuclei over a large range of isospin. The new force SIG-OM with the incompressibility of nuclear matter  $K = 265$  MeV describes the breathing-mode monopole resonance energies very well. A comparative analysis of breathing-mode monopole resonance energies in the RMF theory suggests a smaller value of the surface incompressibility with SIG-OM. The equation of state of nuclear and neutron matter with the new Lagrangian is significantly softer than those with non-linear scalar self-couplings.

We thank Prof. Lev Savushkin for fruitful discussions.

- 
- [1] B.D. Serot and J.D. Walecka, *Adv. Nucl. Phys.* **16** (1986) 1.
  - [2] P.G. Reinhard, *Rep. Prog. Phys.* **52** (1989) 439.
  - [3] B.D. Serot, *Rep. Prog. Phys.* **55** (1992) 1855.
  - [4] Y.K. Gambhir, P. Ring, and A. Thimet, *Ann. Phys. (N.Y.)* **198** (1990) 132.
  - [5] M.M. Sharma, M.A. Nagarajan and P. Ring, *Phys. Lett. B* **312** (1993) 377.
  - [6] G.A. Lalazissis, J. König, and P. Ring, *Phys. Rev. C* **55** (1997) 540.
  - [7] M.M. Sharma, G.A. Lalazissis, and P. Ring, *Phys. Lett. B* **317** (1993) 9.
  - [8] M.M. Sharma, G.A. Lalazissis, J. König, and P. Ring, *Phys. Rev. Lett.* **74** (1994) 3744.
  - [9] P.-G. Reinhard and H. Flocard, *Nucl. Phys.* **A584** (1995) 467.

- [10] J. Boguta and A.R. Bodmer, Nucl. Phys. **A292** (1977) 413.
- [11] M.M. Sharma, A.R. Farhan and S. Mythili, Phys. Rev. C **61** (2000) 054306.
- [12] B.A. Nikolaus, T. Hoch, and D.G. Madland, Phys. Rev. C **46** (1992) 1757.
- [13] J.J. Rusnak and R.J. Furnstahl, Nucl. Phys. **A626** (1997) 495.
- [14] S. Typel and H.H. Wolter, Nucl. Phys. **A656** (1999) 331.
- [15] S. Typel, Phys. Rev. C **71** (2005) 064301.
- [16] T. Niskic, D. Vretenar, P. Finelli and P. Ring, Phys. Rev. C **66** (2002) 024306.
- [17] W. Long, J. Meng, N. Van Giai and S.G. Zhou, Phys. Rev. C **69** (2004) 034319.
- [18] H. Toki, H. Shen, K. Suniyoshi, H. Sugahara and I. Tanihata, J. Phys. G: Nucl. Part. Phys. **24** (1998) 1479.
- [19] B.D. Serot, in *Lecture Notes in Physics* Vol. 641, (Springer Verlag, 2004) p. 31.
- [20] R.J. Furnstahl, B.D. Serot, and H.B. Tang, Nucl. Phys. A **615** (1997) 441.
- [21] L.N. Savushkin et al, Phys. Rev. C **55** (1997) 167.
- [22] B.G. Todd-Rutel, J. Pieckarewicz, Phys. Rev. Lett. **95** (2005) 122501.
- [23] G. Audi and A.H. Wapstra, Nucl. Phys. **A595** (1995) 409.
- [24] E.W. Otten, in *Treatise on Heavy-Ion Science*, edited by D.A. Bromley (Plenum, New York, 1989) Vol 7, p. 517.
- [25] B. Jurado et al., Phys. Lett. B (2007), doi:10.1016/j.physletb.2007.04.006
- [26] G. Sikler et al., Nucl. Phys. **A763** (2005) 45.
- [27] U. Hager et al., Phys. Rev. Lett. **96** (2006) 122501.
- [28] M.M. Sharma, (unpublished, 2007)
- [29] M.V. Stoitsov, P. Ring and M.M. Sharma, Phys. Rev. **C50** (1994) 1445.
- [30] D.H. Youngblood, H.L.Clark, Y.W. Lui, Phys. Rev. C **69** (2004) 034315.
- [31] M.M. Sharma et al., Phys. Rev **C38** (1988) 2562.
- [32] B. Friedman and V.R. Pandharipande, Nucl. Phys. **A361** (1981) 502.